Hindawi
Journal of Nanomaterials
Volume 2019, Article ID 5957606, 9 pages
https://doi.org/10.1155/2019/5957606

Research Article

Development of a Hybrid Chitosan- and Niacinamide-Coupled ZnO Nanoparticle Composite for Sun Protection Application

Hyun-jun Jo,[1] Sang-Myoung Joo,[2] Jeong Yup Kim,[2] Kook-Hyun Yu,[2] and Sang Wook Kim [1]

[1]*Department of Advanced Materials Chemistry, College of Science and Technology, Dongguk University-Gyeongju, Gyeongbuk 38066, Republic of Korea*
[2]*Department of Chemistry, College of Natural Sciences, Dongguk University-Seoul, Seoul 04620, Republic of Korea*

Correspondence should be addressed to Sang Wook Kim; swkim@dongguk.ac.kr

Received 2 May 2019; Accepted 8 October 2019; Published 16 November 2019

Guest Editor: Biaolin Peng

Zinc oxide nanoparticles (ZnO) have long been utilized as UV-protective sunscreen components due to their high durability and lower skin irritation while maintaining capability for blocking UV rays. However, the dispersal and transparency properties of ZnO need to be enhanced in order to improve the capacity for creating effective sunscreen through control of the physiochemical properties of ZnO. In this study, chitosan or niacinamide, which are suitable functional cosmetic compounds and effective skin lightening agents, are combined with ZnO for the development of better UV-protective products. Each biocompatible coating material is individually attached on its surface after the synthesis of ZnO. The size is 70 nm using the sol-gel method. Their morphology and chemical structure are characterized by FT-IR, XRD, SEM, TEM, TGA, and zeta potential. The results indicate that approximately 50% of chitosan and 5% niacinamide were coated on the ZnO. To confirm the capacity of each surface-coated ZnO with chitosan and niacinamide as a sunscreen, we measured their transmission, reflectance, and sun protection factor (SPF) using a UV spectrophotometer and SPF. As a result, the niacinamide-coated ZnO shows remarkably lower transmission and high reflectance against UV rays than that of bare ZnO and chitosan-coated ZnO. Furthermore, niacinamide-coated ZnO exhibits great lightening effects. Consequently, these results demonstrate that niacinamide coating is highly effective for the production of sunscreen emulsions.

1. Introduction

Ultraviolet (UV) rays are categorized into 3 different types: UV-A (320-400 nm), UV-B (280-320 nm), and UV-C (200-290 nm). When UV rays are exposed to a 200-400 nm wavelength area of sunlight, they can cause skin diseases such as skin cancer and premature aging. Sunscreen emulsion is defined as a skin protectant against UV rays. Exposure to UV-A radiation leads to damage to the elastic and collagenic fibers of connective tissue of skin, which leads to premature aging (photoaging). Furthermore, UV-B radiation causes acute inflammation (sunburn) and intensification of photoaging [1–5]. Organic sunscreen absorbs UV rays and then transfers either infrared rays or heat energy. For example, benzoic acid ester types and benzophenone types such as cinnamate and p-aminobenzoic are often present in organic sunscreen. Although these organic materials have excellent sunscreen attributes, there are some disadvantages. For example, the UV wavelength protection is narrow, skin irritation is common, and effective sunburn resistance is poor [6, 7].

When used in sunscreen emulsion, inorganic materials such as zinc oxide (ZnO) have several attributes. Inorganic sunscreen scatters UV rays with components that have a wide protective area. It has higher durability and lower skin irritation than organic materials. Due to ZnO's low refractive index compared to that of titanium dioxide (TiO_2), it can reduce the appearance of a white cast. As TiO_2 generates oxygen free radicals, it causes damage to skin cells and neuron cells which are harmful to the body. Furthermore, ZnO is nontoxic, has optically active attribution, and is both physically and chemically secure. It is also used in fabric, photocatalysis, and electronic industries as well as in the manufacturing of medical supplies. ZnO has a high exciton binding energy (60 meV). Also, because it has the band gap

energy of 3.22 eV, ZnO can protect against the range of UV-A (320~400 nm) [2, 5, 8–10].

Typically, in the case of metal oxide nanoparticles, the attribution is known to be size dependent. Smaller ZnO nanoparticles are more efficient at protecting against harmful UV rays. The optimal size of ZnO nanoparticles is 40-70 nm, which results in effective absorbance and high band gap energy. When the particles' sizes are smaller than 40 nm, the protective absorbance decreases and the band gap energy increases. Therefore, the particles have to be at least 40 nm in size [11–19].

Although ZnO has an excellent protective effect in its nanoparticles status, there are some disadvantages. For example, it is difficult for ZnO nanoparticles to disperse, the particles are aggregative, and also the white cast the produce would be visible due to reflection of radiation. To compensate aggregation and white cast, chitosan and niacinamide (natural organic materials) are utilized to synthesize chitosan (CS)/ZnO and niacinamide (Nia)/ZnO composites.

Chitosan resulted from processing chitin with alkali, a glucosamine polymer. Chitosan is comprised of glucosamine binding, and the molecule structure of chitosan is very similar to that which is found in the human body. Furthermore, it is friendly to the body and nontoxic. It has high moisturization and dispersibility capacity, which are suitable for functional cosmetic compounds [20–23].

Niacinamide is a functional natural organic material. In the body, niacinamide is a component of nicotinamide adenine dinucleotide (NAD) (also known as coenzyme I) and nicotinamide adenine dinucleotide phosphate (NADP) (also recognized as coenzyme II). These coenzymes are involved in many intracellular oxidation-reduction reactions. As a result, niacinamide is used as an antioxidant. Niacinamide has been effective on the treatment of cutaneous hyperpigmentation. In clinical trials, the niacinamide moisturizer provides inhibition of melanosome shift from melanocytes to keratinocytes, proving to be an effective skin lightening agent [23–25].

In this study, ZnO is synthesized to 70 nm using the sol-gel method in order to provide nontoxicity, boost up dispersion, and reduce a white cast. Synthesized ZnO nanoparticles were coupled with natural organic chitosan and niacinamide by modifying the surface to achieve CS/ZnO and Nia/ZnO.

The prepared chitosan- and niacinamide-associated ZnO nanoparticle compounds gave excellent UV protection activity.

2. Method

As a precursor, zinc oxide nanoparticles were prepared using zinc acetate. The surface of synthesized ZnO NPs was modified using either chitosan or niacinamide. Reagents for synthesis were used without a refining process. Zinc acetate dihydrate, oxalic acid dihydrate (99.5%), niacinamide, and medium molecular weight chitosan were purchased from Sigma-Aldrich, USA. The second group (acetic acid glacial (99.5%), ethyl alcohol anhydrous (99.9%), and sodium hydroxide) was purchased from Daejung Chemical, Korea.

Table 1: Formula for W/O emulsion.

Material name	Content (%)	Phase
Liquid paraffin	34	Oil phase
Olivem 900	5	
ZnO, CS/ZnO, Nia/ZnO	5	
Sodium chloride	2	Water phase
Water	To 100	

Structural analysis of synthesized materials verified functional groups using the following analysis methods: Fourier transform infrared spectroscopy (Tendo 30 of the company, Bruker, USA), X-ray diffraction (Ultima IV X-ray diffractometer, Rigaku Corporation, USA), field-emission scanning electron microscopy energy-dispersive spectroscopy (SU-8010, Hitachi, Japan), biotransmission electron microscopy (HT 7700, Hitachi, Japan), thermogravimetric analysis (STA 6000, PerkinElmer, USA), and dynamic light scattering-zeta potential (Zetasizer Nano ZS90, USA). Transmission ratio and reflectance of synthesized materials are confirmed by ultraviolet-visible spectroscopy (Carry 4000, Varian Corporation). Sun protection factor was measured using a UV Sunscreen Analyzer (UV-2000S, Labsphere, USA).

2.1. Synthesis of Materials

2.1.1. The Synthesis of ZnO. Zinc acetate (5.01 mmol) and 300 mL ethyl alcohol are stirred at 50°C for an hour using a reflux system. Typically, the oxalic acid (14 mmol) was dissolved in 200 mL ethyl alcohol, followed by the dissolved addition of zinc acetate to the above mixture (5.01 mmol, ethyl alcohol 300 mL). The mixture was stirred at 50°C in a reflux system for 1 h. The gel of ZnO was cooled down to room temperature, and it was dried at 70°C in the oven for 20 min. Afterwards, it was sintered at 650°C for 4 h using an electric furnace [26].

2.1.2. The Synthesis of Chitosan-Integrated ZnO. The surface of ZnO was modified into CS/ZnO by the following steps. Initially, ZnO (0.1 g) was stirred in 100 mL of 1% acetic acid solution. Later, 0.1 g of chitosan was transferred into the dissolved ZnO solution, and the combination of chitosan (0.1 g) and the dissolved ZnO was sonicated for 30 min. Next, 1 M of sodium hydroxide was added into the above mixture (pH 10). It was kept at 60°C and stirred for 3 h. Later, the gel was washed with distilled water several times and dried at 50°C for 3 hours [23].

2.1.3. The Synthesis of Niacinamide-Integrated ZnO. ZnO (0.1 g) was added to ethyl alcohol (3.17 mL) and stirred at 700 rpm at 25°C for 20 min. The mixture of sodium hydroxide (0.01 g) and ethyl alcohol (0.25 mL) was added to the above solution and stirred for 20 min. It was dispersed using sonication for 30 min. The dispersed ZnO was stirred at 700 rpm at 75°C for 30 min. The mixture of niacinamide (0.25 g) and ethyl alcohol (0.32 mL) was added to the dispersed ZnO solution, and it was stirred at 700 rpm at 75°C for 3 h. The resultant solid was washed with ethyl alcohol several times and dried in a vacuum.

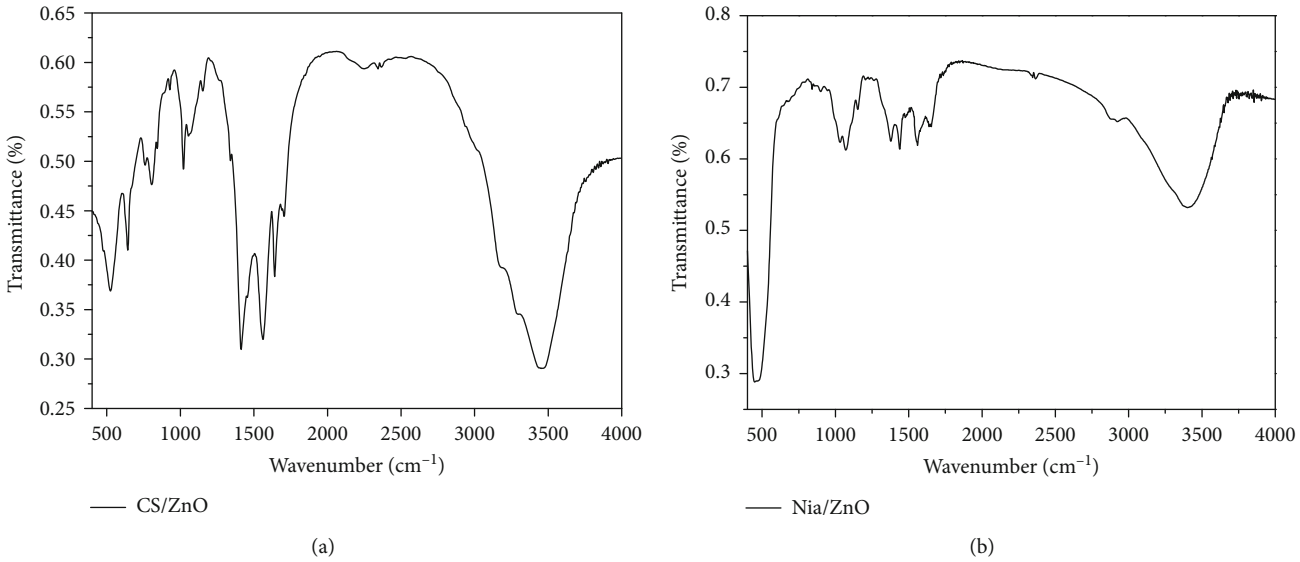

Figure 1: FT-IR spectra of CS/ZnO (a) and Nia/ZnO (b).

2.2. Evaluation of Sunscreen Emulsion Formulation. W/O emulsion was formulated based on the ratio shown in Table 1 so as to confirm the sun protection factor (SPF) of ZnO, CS/ZnO, and Nia/ZnO. The water phases consist of dissolved sodium chloride into water at 80°C. Next, the oil phase is formulated. Olivem 900 and liquid paraffin are mixed at 80°C. This mixture is divided into three parts, with each part added to the synthesized ZnO, CS/ZnO, and Nia/ZnO, respectively, at 80°C. The water phase and oil phase were mixed, and the mixture was dispersed for 30 minutes [27].

2.3. Tyrosinase Inhibition Assay. A variety of concentrated samples of 20 μL and 0.1 M phosphate buffer (100 μL) were mixed and reacted for 5 minutes at room temperature. 1 k unit/mℓ of tyrosinase (in 0.1 M phosphate buffer) (30 μL) and 1.5 mM tyrosine (30 μL) were mixed for 10 min at 37°C, and the enzyme reaction was proceeded.

The absorbance was measured at 490 nm of wavelength after the completion of reaction. Based on the standard of the inhibition assay, 0.1 M phosphate buffer was added instead of the samples. For comparative analysis, arbutin was used as a positive control.

2.4. Cell Viability. The culture medium consists of 10% heat-inactivated fetal bovine serum, 100 units/mL penicillin, and 100 μg/mL streptomycin. The melamine cell (SK-MEL-28) was incubated with the formulated culture medium in the cell plate, then incubated at 5% of CO_2 at 37°C. The culture medium mixture and melamine cell (SK-MEL-28) were moved to the three different well plates. ZnO, CS/ZnO, and Nia/ZnO were added into each well plate. When this procedure was completed, incubated cells were moved to each well plate. After 24 hours, the culture medium was removed. Then, 100 μL of MTT (5 mg/mL in PBS) was added into the well plate at 5% of CO_2 at 37°C for 2-3 hours. This caused some of the MTT to react, thereby transforming it into a burgundy-colored formazan. Next, the excess MTT that did not react was removed. Later, DMSO was added to the formazan/SK-MEL-28 well plate, and the mixture was shaken for 15-20 min. 540 nm of the absorbance was measured upon analysis [28, 29].

3. Results and Discussion

3.1. Characterization of CS/ZnO and Nia/ZnO

3.1.1. Fourier Transform Infrared Spectroscopy. The IR spectra of CS/ZnO were confirmed that the -OH and -NH groups displayed a stretching vibration of its bands from 3400 to 3250 cm^{-1}. The band at 2876 cm^{-1} is assigned to the asymmetric stretching vibration of the -CH group. 1650 cm^{-1} shows a stretching vibration of N-H while 1424 cm^{-1} demonstrates C-N and 1047 cm^{-1} indicates C-O-C of the band. As the result of the spectra, the synthesis of CS/ZnO is validated by the results (Figure 1(a)).

The IR spectra of Nia/ZnO display both an OH peak and NH peak of the stretching vibration at 3600~3100 cm^{-1} band. The C-H peak of the stretching vibration reads 2850~3000 cm^{-1}, and the peak of C=O of the stretching vibration is displayed at 1650~1700 cm^{-1}. The NH peak of the stretching vibration is indicated at 1600~1650 cm^{-1}, and C-N of the stretching vibration reads 1335~1250 cm^{-1}. Therefore, the synthesis of Nia/ZnO was confirmed by FTIR analysis (Figure 1(b)).

3.1.2. X-Ray Diffraction Analysis. The XRD pattern of ZnO (ICDD card 01-075-0576) is verified, and the crystal face is confirmed as a hexagonal structure. The crystal faces of CS/ZnO and Nia/ZnO, which result from the synthesis of CS and Nia with ZnO, respectively, confirm the identical crystal face of ZnO, as shown in Figure 2.

3.1.3. Scanning Electron Microscope (SEM). Figure 3(a) shows that the particle size of ZnO is 65~80 nm. The ZnO's particle shape displays the characteristics of a hexagonal structure. The ZnO analysis results using the EDS confirm the ingredients of both zinc and oxygen as shown in Table 2.

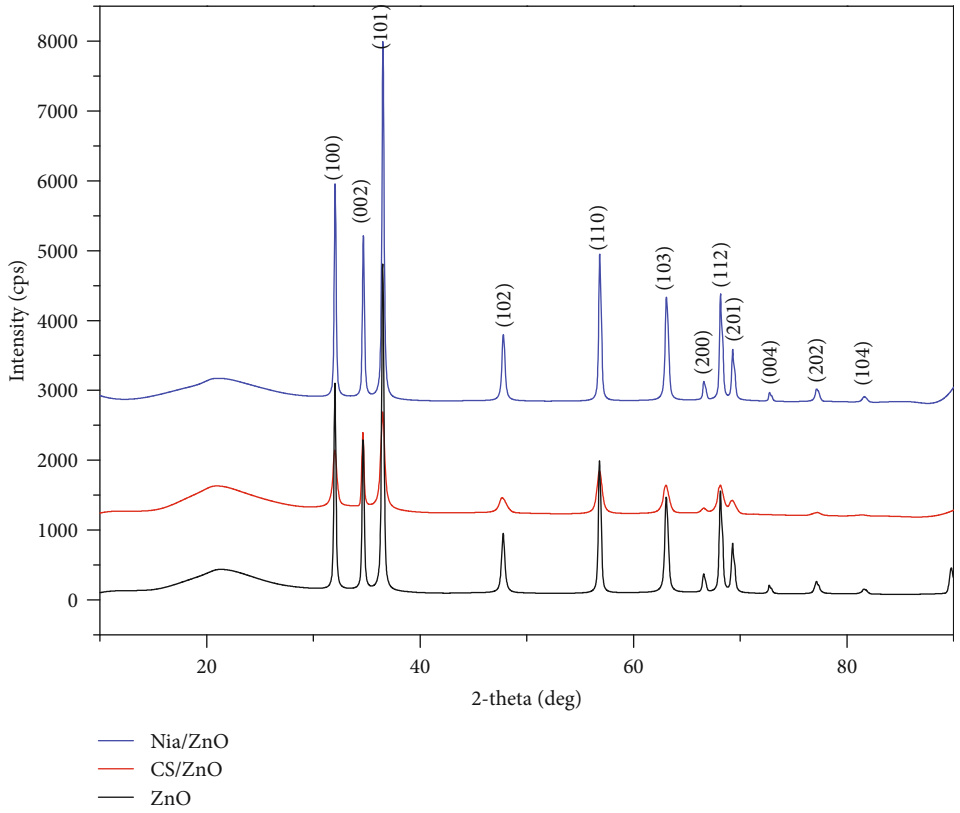

Figure 2: X-ray diffraction pattern of ZnO, CS/ZnO, and Nia/ZnO. This shows the results of X-ray diffraction analysis. The bottom line in black shows the pattern of ZnO, the middle one in red illustrates the pattern of CS/ZnO, and the top one in blue displays the pattern of Nia/ZnO.

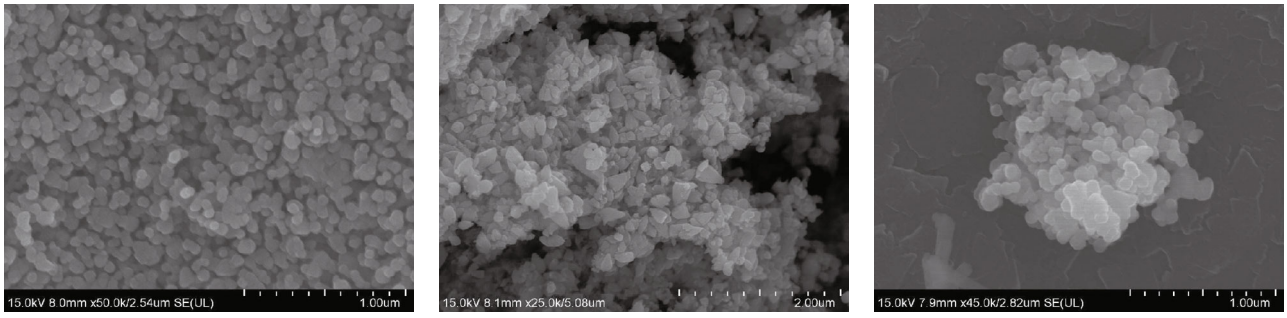

(a) (b) (c)

Figure 3: SEM images of ZnO (a), CS/ZnO (b), and Nia/ZnO (c). The measurements were processed with a platinum pretreatment of ZnO (a), CS/ZnO (b), and Nia/ZnO (c).

The particle size of CS/ZnO is between 150 and 180 nm as indicated in Figure 3(b). The SEM image of CS/ZnO has a rough surface as compared to that of ZnO. EDS results confirm the binding of chitosan with ZnO nanoparticles.

The SEM image proves the size of Nia/ZnO between 90 and 100 nm, as indicated in Figure 3(c). As mentioned previously, the EDS analysis confirms that zinc and oxygen combine to form ZnO. Furthermore, it was found that Nia/ZnO was coated with niacinamide, as shown in Table 2. The results exhibited that chitosan and niacinamide are associated with ZnO.

Table 2: The composites were analyzed by energy-dispersive spectroscopy.

	Wt (%)		
	ZnO	CS/ZnO	Nia/ZnO
Zinc	80.17	58.50	17.82
O	13.34	18.37	49.53
C	—	17.14	27.12
N	—	2.48	2.32
Pt	6.49	3.51	3.21
Total	100.00	100.00	100.00

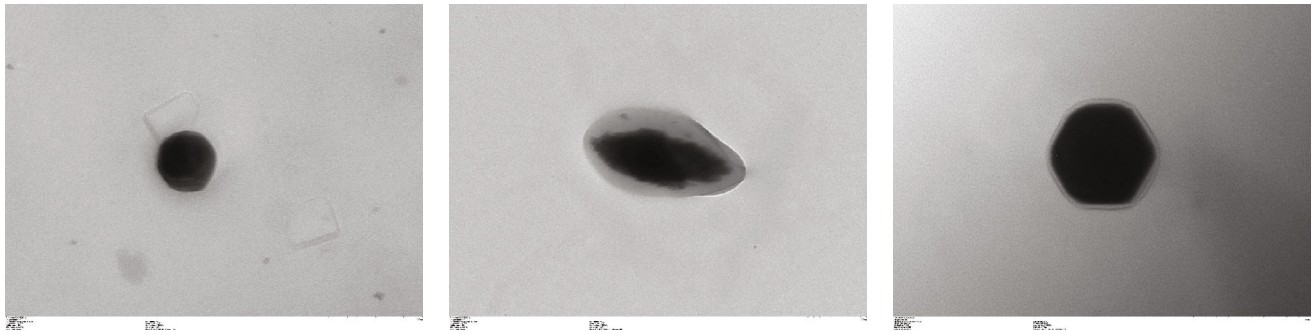

(a) (b) (c)

Figure 4: TEM images of ZnO (a), CS/ZnO (b), and Nia/ZnO (c). The measurements are processed with a chloroform pretreatment of ZnO (a), CS/ZnO (b), and Nia/ZnO (c).

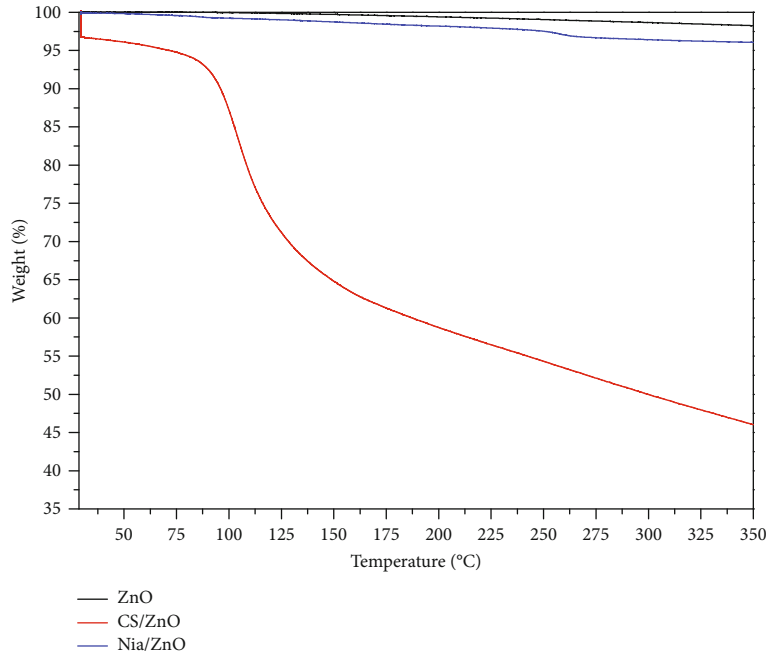

Figure 5: Thermogravimetric analysis of ZnO, CS/ZnO, and Nia/ZnO. These three samples, 50 mg each, are subjected to heat, specifically 10°C per minute. The thermogravimetric analysis was completed when each sample was subjected to a temperature of 350°C. The numbers on the left of the graph show the percentage of weight loss. The black line shows the weight loss of pure ZnO (to be referred to as ZnO from this point forward), the red line illustrates the Nia/ZnO weight loss, and the blue line displays the CS/ZnO weight loss.

3.1.4. Transmission Electron Microscope (TEM). The TEM images show the dispersal of each sample in chloroform on a nickel grid. The samples are dissolved in chloroform through sonication for 30 minutes. After this is completed, the three grids are absorbed and dried for an additional 30 minutes. ZnO nanoparticles are shown in Figure 4(a). On the other hand, when the TEM images are confirmed as to whether or not the organic material is introduced, they show that chitosan and niacinamide are sufficiently covered with organic materials in Figures 4(b) and 4(c). When the organic layers of chitosan are observed, many organic layers are confirmed by the TEM images, which means that the organic layers of chitosan are largely covered. In comparison, niacinamide is found to be coated as thin as the composite ratio of 5% niacinamide/95% ZnO.

Table 3: Dynamic light scattering-zeta potential.

	DLS (nm)	Zeta potential (mV)
ZnO	95.07	-2.81
CS/ZnO	86.60	10.4
Nia/ZnO	95.07	-32.3

3.1.5. Thermogravimetric Analysis. The differences between ZnO, CS/ZnO, and Nia/ZnO confirm the organic layers as seen in Figure 4. The purpose of conducting thermogravimetric analysis is to determine the composite ratio of organic weight loss with respect to these three materials. When the temperature of ZnO increased in thermogravimetric analysis, the weight loss was not considerable. This means that ZnO is highly stable under extreme heat, up to 1975°C. However,

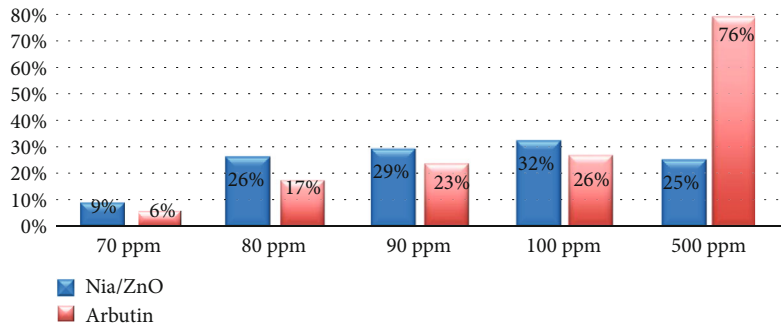

Figure 6: Concentrations of tyrosinase inhibitory activity of Nia/ZnO and arbutin. Arbutin was used as the positive control of Nia/ZnO. When concentration increased, the samples were not dissolved, which led to the measurement value being significantly lower than that of the positive control.

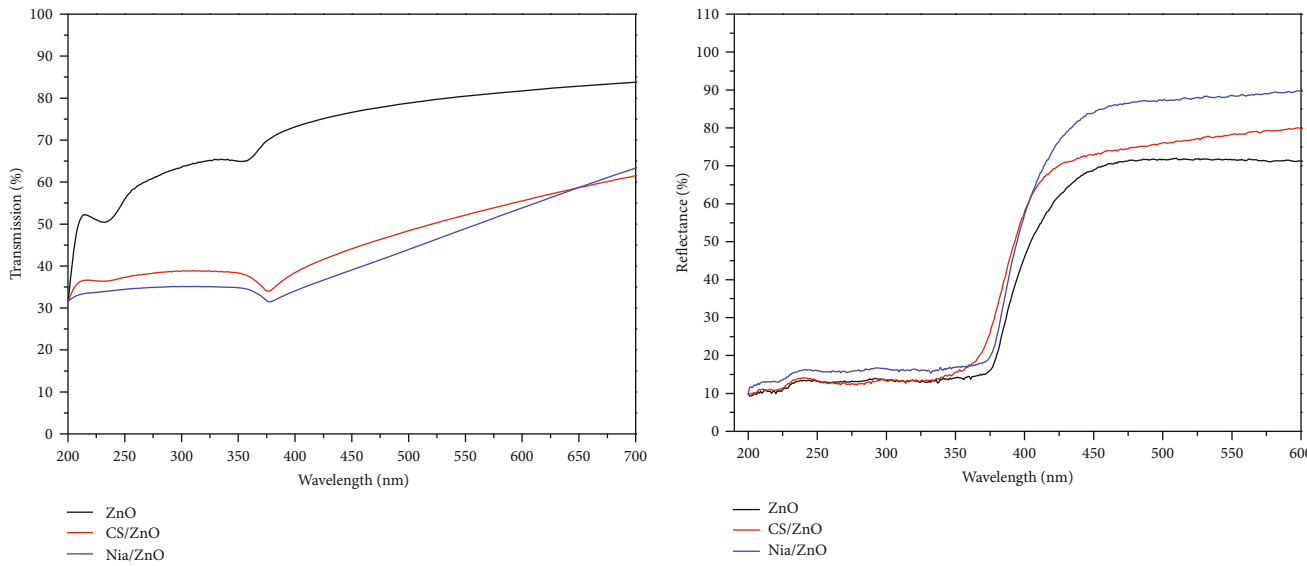

(a) (b)

Figure 7: UV-visible transmission (a) of and reflectance (b) spectra of ZnO, CS/ZnO, and Nia/ZnO. After the three samples were dissolved into the 0.01% distilled water, they were scanned at 200~800 nm by ultraviolet-visible spectroscopy.

because of the water molecules present in chitosan, the CS/ZnO polymer displayed a two-phase weight loss. The first phase resulted in a weight loss of water at under 100°C. The final decline of polymer occurred at the point between 110 and 325°C. The composite ratio of chitosan and ZnO is 50/50, meaning that 50% of each sample was used. In order to confirm the ratio, the weight loss of chitosan was monitored. As a result, all of the chitosan evaporated during this process. The remaining ratio of the CS/ZnO (now just ZnO is remaining) was 50%, which confirms that the ratio was accurate. In the case of Nia/ZnO, the composite ratio of 5% Nia and 95% ZnO was used. The 5% decrease refers to the niacinamide coating which was a result of the synthesis experiment in Section 2.3. Based on the results, a small thermal change at 250°C occurred and the weight loss was observed at the end. Niacinamide was stable until it reached 235°C, but decreased in weight by 5% at 276°C. The remaining 95% consists entirely of ZnO.

The results in Figure 5 display clear comparisons between ZnO, CS/ZnO, and Nia/ZnO with regard to their weight loss under thermogravimetric analysis. Thermogravimetric analysis of ZnO shows that the weight loss of ZnO only slightly occurs at high temperatures. Furthermore, CS/ZnO exhibits significant weight loss at around 100°C until the chitosan completely disappears at 350°C. Lastly, Nia/ZnO lost all of the niacinamide, but not until it reached a heat of 276°C. Therefore, Nia/ZnO, with its lower composite ratio and higher stability under heat, is far more effective than CS/ZnO, which has a higher composite ratio and lower stability under heat. Further studies involving UV and SPF are discussed in Sections 3.1.8 and 3.1.9.

3.1.6. Dynamic Light Scattering- (DLS-) Zeta Potential Study. Table 3 indicates that the dispersed particle sizes of Zn, CS/ZnO, and Nia/ZnO are 95.07 nm, 86.60 nm, and 95.07 nm based on the DLS measurement result, respectively.

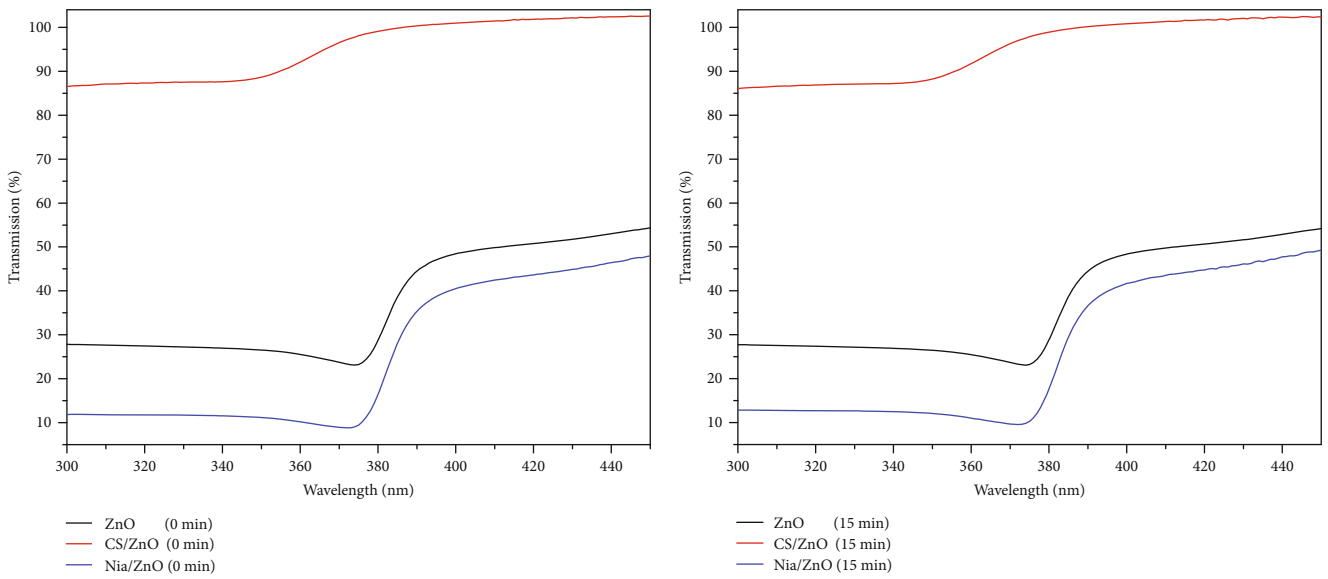

Figure 8: SPF activity of ZnO, CS/ZnO, and Nia/ZnO with time. The emulsions which was prepared for the experiment method of the previous part (Section 2.2) were applied on the cell plates and measured at UV-2000 300 mg/cm^3.

As a result, the zeta potential of CS/ZnO (10.4 mV) and Nia/ZnO (-32.3 mV) was higher than that of the pure ZnO nanoparticle (-2.81 mV).

3.1.7. Tyrosinase Assay Ratio. Tyrosinase stimulates the significant process of generating melanin in the skin cell. When melanin is excessively pigmented, it causes skin aging. The tyrosinase experiment that prohibits tyrosinase reaction is usually used for studies on the effects of skin lightening.

Under the tyrosinase experiment, tyrosinase inhibitory activity is not measured from ZnO and CS/ZnO materials while tyrosinase inhibitory activity is accomplished from the Nia/ZnO composite and has a lightening effect. The tyrosinase inhibitory activity of Nia/ZnO is measured at different concentrations (Figure 6). The higher concentration of Nia/ZnO produced more inhibitory activity increases. When the sample over 500 ppm concentration is dispersed, the dispersion of the nanoparticles did not occur. Therefore, the experiment was performed at a lower concentration than the inhibitory activity of the positive control. The positive control of tyrosinase inhibitory activity is confirmed by using arbutin. The results of the measurement demonstrate that upon increment of amount of the tyrosinase assay of Nia/ZnO, the tyrosinase inhibitory activity increases. Therefore, the lightening effects of Nia/ZnO are confirmed [30–33].

3.1.8. Ultraviolet-Visible Spectroscopy. In order to measure transmission, 0.001% of each ZnO, CS/ZnO, and Nia/ZnO sample was dispersed in distilled water. The result of this experiment shows that transmission of the synthesized materials, CS/ZnO and Nia/ZnO, is lower than the transmission of ZnO (Figure 7(a)). The difference of transmission between the pure ZnO and CS/ZnO is 34.7%, and the difference of transmission between the pure ZnO and Nia/ZnO was 39% in the UV ray range (200-400 nm). The transmission difference between CS/ZnO and Nia/ZnO was 4.3% in the same UV ray range. On the other hand, the reflectance differences between the pure ZnO, CS/ZnO, and Nia/ZnO were not significant, as shown in Figure 7(b). The reflectance difference between ZnO and CS/ZnO is 3%, and the reflectance difference between ZnO and Nia/ZnO is 15.1% in the visible ray region. However, CS/ZnO and Nia/ZnO have 2.8% and 3% reflectance with respect to ZnO, which is lower in the UV ray region.

Table 4: SPF timed mean study of ZnO, CS/ZnO, and Nia/ZnO.

	SPF mean	*T* (UVA)	*T* (UVB)	Lambda critical
ZnO 0 min	4.06	0.3023	0.2769	383.2
ZnO 15 min	4.11	0.3019	0.2762	383.1
CS/ZnO 0 min	1.15	0.9325	0.8869	355.3
CS/ZnO 15 min	1.18	0.9293	0.8823	356
Nia/ZnO 0 min	8.83	0.1653	0.1184	380.3
Nia/ZnO 15 min	9.96	0.1658	0.1187	380.2

3.1.9. Sun Protection Factor (SPF). The sunscreen emulsions were formulated as previously described in Section 2.2. The SPF mean of each sunscreen emulsion in UV-2000 was studied as shown in Figure 8 and Table 4. The measurement was carried out at 0 min and 15 min. As a result, the CS/ZnO and Nia/ZnO emulsions show remarkable UV ray protection efficiency compared to the ZnO emulsion. However, CS/ZnO was proven as not being able to function as an effective sunscreen emulsion for two reasons. (i) The transmission of CS/ZnO was significantly higher than that of ZnO, which means that CS/ZnO transmitted more than 90% of UV rays. (ii) Also, the SPF mean for CS/ZnO showed to be 1.18

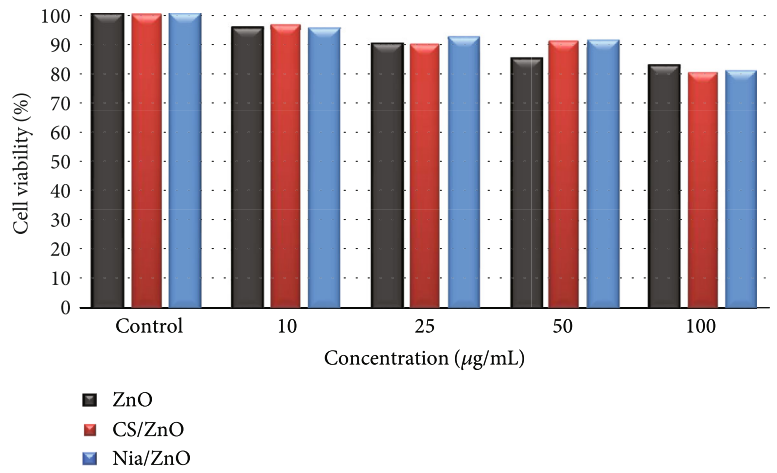

Figure 9: Cell viability of ZnO, CS/ZnO, and Nia/ZnO. The graph shows the result of the MTT experiment which in the three samples was carried out by using the skin cell (SK-Mel-28). The concentration shown in the graph is generally used for the nanoparticles.

(15 min), which was the lowest among the three materials. Nia/ZnO, on the other hand, measured an SPF mean of 9.96 at 15 min and has a UV ray transmission of 16%, which is more efficient than that of pure ZnO.

3.1.10. Cell Viability. As ZnO, CS/ZnO, and Nia/ZnO can be used as sunscreen emulsions, it was concluded that their nanoparticles were cytotoxic to the skin using the cell viability. The cell viability of ZnO, CS/ZnO, and Nia/ZnO was tested using a specific skin cell (SK-Mel-28) [34–36]. When the concentration of nanoparticles was exposed at 100 μg/mL, more than 80% of cells survived (Figure 9). This concentration (100 μg/mL) is used for the nanoparticle MTT assay. The high survival rate was displayed at the highest concentration. The poison did not show a significant difference in this concentration.

4. Conclusion

In the present study, chitosan and niacinamide, natural organic materials, play an important role as components of functional cosmetics. They each have a skin dispersible capacity, provide high levels of moisture, and are mild to the skin. With these benefits, chitosan and niacinamide should be synthesized with ZnO nanoparticles for maximum effectiveness. Remarkably, 0.18 g of ZnO was yielded through the sol-gel method while 0.17 g of CS/ZnO and 0.08 g of Nia/ZnO were yielded in our experiments. The formation of three synthesized materials (ZnO, CS/ZnO, and Nia/ZnO) was characterized through the use of IR, XRD, FE-SEM-EDS, Bio-TEM, TGA, DLS, and zeta potential technics.

Nia/ZnO was determined to have a lightening effect as a result of the tyrosinase experiment. Also, as the concentrations of ZnO, CS/ZnO, and Nia/ZnO were high under the cell viability, the cell extinction did not display a significant difference. In terms of reflectance properties, pure ZnO did not show a significant difference compared to the UV reflectance properties of CS/ZnO and Nia/ZnO. Due to CS/ZnO and Nia/ZnO showing lower levels of UV transmission than pure ZnO, they are more efficient against UV rays. In the SPF mean study, more than 90% of CS/ZnO was transmitted through UV rays, which indicates that CS/ZnO is not as efficient as ZnO. However, the transmission of Nia/ZnO was lower than that of pure ZnO while maintaining a higher SPF mean than that of pure ZnO, resulting in Nia/ZnO being the most effective compound for sunscreen lotion. Furthermore, UV transmission and SPF experiments suggested that Nia/ZnO outperformed both ZnO and CS/ZnO. Furthermore, Nia/ZnO was the only compound to produce a lightening effect.

Data Availability

The data used to support the findings of this study are included within the article.

Conflicts of Interest

The authors declare that they have no conflicts of interest.

Acknowledgments

This study was supported by the National Research Foundation Grant funded by the Korean Government (2017R1D1A1B03035589) and Dongguk University-Gyeongju Research Fund 2019.

References

[1] M. R. Serafini, C. B. Detoni, P. D. P. Menezes et al., "UVA-UVB Photoprotective Activity of Topical Formulations Containing *Morinda citrifolia* Extract," *BioMed Research International*, vol. 2014, Article ID 587819, 10 pages, 2014.

[2] T. G. Smijs and S. Pavel, "Titanium dioxide and zinc oxide nanoparticles in sunscreens: focus on their safety and effectiveness," *Nanotechnology, Science and Applications*, vol. 4, 2011.

[3] A. Nasu and Y. Otsubo, "Effects of polymeric dispersants on the rheology and UV-protecting properties of complex suspensions of titanium dioxides and zinc oxides," *Colloids and Surfaces A: Physicochemical and Engineering Aspects*, vol. 326, no. 1-2, pp. 92–97, 2008.

[4] V. C. Seixas and O. A. Serra, *Molecules*, vol. 19, no. 7, pp. 9907–9925, 2014.

[5] A. Nasu and Y. Otsubo, "Rheology and UV-protecting properties of complex suspensions of titanium dioxides and zinc oxides," *Journal of Colloid and Interface Science*, vol. 310, no. 2, pp. 617–623, 2007.

[6] C. R. Srinivas and R. Rai, "Photoprotection," *Indian Journal of Dermatology, Venereology, and Leprology*, vol. 73, no. 2, p. 73, 2007.

[7] S. Kale, A. Sonawane, A. Ansari, P. Ghoge, and A. Waje, "Formulation and in-vitro determination of sun protection factor of Ocimum basilicum, Linn. leaf oils sunscreen cream," *International Journal of Pharmacy and Pharmaceutical Sciences*, vol. 2, 2010.

[8] R. Yoshida, "Novel multifunctional zinc oxide for improving makeup cosmetics," *Fragrance Journal Korea*, vol. 1, 2016.

[9] A. Kołodziejczak-Radzimska and T. Jesionowski, "Zinc oxide—from synthesis to application: a review," *Materials.*, vol. 7, no. 4, pp. 2833–2881, 2014.

[10] Z. L. Wang, "Zinc oxide nanostructures: growth, properties and applications," *Journal of Physics: Condensed Matter*, vol. 16, 2004.

[11] H. S. Kil, Y. H. Kim, M. Park, and S. W. Rhee, "Synthesis and Characterization of Mica Coated with Zinc Oxide Nanoparticles," *Applied Chemistry for Engineering*, vol. 23, no. 3, pp. 271–278, 2012.

[12] E. G. Goh, X. Xu, and P. G. McCormick, "Effect of particle size on the UV absorbance of zinc oxide nanoparticles," *Scripta Materialia*, vol. 78, pp. 49–52, 2014.

[13] N. A. Monteiro-Riviere, K. Wiench, R. Landsiedel, S. Schulte, A. O. Inman, and J. E. Riviere, "Safety evaluation of sunscreen formulations containing titanium dioxide and zinc oxide nanoparticles in UVB sunburned skin: an in vitro and in vivo study," *Toxicological Sciences*, vol. 123, no. 1, pp. 264–280, 2011.

[14] R. Vandebriel and W. De Jong, "A review of mammalian toxicity of ZnO nanoparticles," *Nanotechnology, Science and Applications*, vol. 5, 2012.

[15] Z. Cao, Z. Zhang, F. Wang, and G. Wang, "Synthesis and UV shielding properties of zinc oxide ultrafine particles modified with silica and trimethyl siloxane," *Colloids and surfaces A: physicochemical and engineering aspects*, vol. 340, no. 1-3, pp. 161–167, 2009.

[16] H. M. Cheng, H. C. Hsu, S. L. Chen et al., "Efficient UV photoluminescence from monodispersed secondary ZnO colloidal spheres synthesized by sol-gel method," *Journal of Crystal Growth*, vol. 277, no. 1-4, pp. 192–199, 2005.

[17] L. Qin, C. Shing, S. Sawyer, and P. S. Dutta, *Optical Materials*, vol. 33, no. 3, pp. 359–362, 2011.

[18] M. S. Latja, *The Journal of Clinical and Aesthetic Dermatology*, vol. 6, pp. 16–26, 2013.

[19] M. A. Suva, "Evaluation of sun protection factor of Zingiber officinale Roscoe extract by ultraviolet spectroscopy method," *Journal of Pharmaceutical Sciences*, vol. 3, pp. 95–97, 2014.

[20] J. Kumirska, M. X. Weinhold, J. Thöming, and P. Stepnowski, "Biomedical activity of chitin/chitosan based materials—influence of physicochemical properties apart from molecular weight and degree of N-acetylation," *Polymers*, vol. 3, no. 4, pp. 1875–1901, 2011.

[21] M. M. AbdElhady, "Preparation and characterization of chitosan/zinc oxide nanoparticles for imparting antimicrobial and UV protection to cotton fabric," *International Journal of Carbohydrate Chemistry*, vol. 2012, Article ID 840591, 6 pages, 2012.

[22] M. Thirumavalavan, K. L. Huang, and J. F. Lee, "Preparation and morphology studies of nano zinc oxide obtained using native and modified chitosans," *Materials*, vol. 6, no. 9, pp. 4198–4212, 2013.

[23] Y. Haldorai and J. J. Shim, "Chitosan-zinc oxide hybrid composite for enhanced dye degradation and antibacterial activity," *Composite Interfaces*, vol. 20, no. 5, pp. 365–377, 2013.

[24] *Alternative Mediecine Review*, vol. 7, p. 525, 2002.

[25] F. Lin, W. Xu, C. Guan et al., "Niacin protects against UVB radiation-induced apoptosis in cultured human skin keratinocytes," *International Journal of Molecular Medicine*, vol. 29, no. 4, pp. 593–600, 2012.

[26] H. Benhelbal, "IFC - Editorial Board," *Alexandria Engineering Journal.*, vol. 52, 2013.

[27] C. K. Zhoh, H. J. Kwon, and S. R. Ahn, "The Optical Characteristics of Titanium Dioxide and UV-block Effect," *Korean Journal of Aesthetics and Cosmetics Society*, vol. 9, no. 2, 2011.

[28] S. Tao, S. L. Park, M. R. De La Vega, D. D. Zhang, and G. T. Wondrak, "Systemic administration of the apocarotenoid bixin protects skin against solar UV-induced damage through activation of NRF2," *Free Radical Biology and Medicine*, vol. 89, pp. 690–700, 2015.

[29] M. Ramani, M. C. Mudge, R. T. Morris et al., "Zinc Oxide Nanoparticle–Poly I:C RNA Complexes: Implication as Therapeutics against Experimental Melanoma," *Molecular Pharmaceutics*, vol. 14, no. 3, pp. 614–625, 2017.

[30] B. X. Gu, C. X. Xu, G. P. Zhu, S. Q. Liu, L. Y. Chen, and X. S. Li, "Tyrosinase Immobilization on ZnO Nanorods for Phenol Detection," *The Journal of Physical Chemistry B*, vol. 113, no. 1, pp. 377–381, 2009.

[31] D. Y. Im and K. I. Lee, "Antioxidative activity and tyrosinase inhibitory activity of the extract and fractions from Arctium lappa roots and analysis of phenolic compounds," *Korean Journal of Pharmacognosy*, vol. 45, pp. 141–146, 2014.

[32] V. del Marmol and F. Beermann, *FEBS Letters*, vol. 381, no. 3, pp. 165–168, 1996.

[33] S. W. Jung, N. K. Lee, S. J. Kim, and D. S. Han, "Screening of tyrosinase inhibitor from plants," *Korean Journal of Food Science and Technology*, vol. 27, pp. 891–896, 1995.

[34] R. Jiang, H.-Y. Zhu, H.-H. Chen et al., "Effect of calcination temperature on physical parameters and photocatalytic activity of mesoporous titania spheres using chitosan/poly(vinyl alcohol) hydrogel beads as a template," *Applied Surface Science*, vol. 319, pp. 189–196, 2014.

[35] H. S. Joung, "Antimelanogenic effect of taurine in murine melanoma B16F10 cells," *The Pharmaceutical Society of Korea*, vol. 51, pp. 350–354, 2007.

[36] M. Orazizadeh, A. Khodadadi, V. Bayati, S. Saremy, M. Farasat, and L. Khorsandi, "*In Vitro* Toxic Effects of Zinc Oxide Nanoparticles on Rat Adipose Tissue-Derived Mesenchymal Stem Cells," *Cell Journal*, vol. 17, no. 3, pp. 412–421, 2015.